Chinese Chemical Letters 34 (2023) 107445

Contents lists available at ScienceDirect

Chinese Chemical Letters

journal homepage: www.elsevier.com/locate/cclet

Tetradentate cyclometalated platinum complex enables high-performance near-infrared electroluminescence with excellent device stability

Chengjun Wu[a], Youming Zhang[a,b,*], Jingsheng Miao[a,*], Kai Li[a], Weiguo Zhu[b], Chuluo Yang[a,*]

[a] Shenzhen Key Laboratory of New Information Display and Storage Materials, Guangdong Research Center for Interfacial Engineering of Functional Materials, College of Materials Science and Engineering, Shenzhen University, Shenzhen 518055, China
[b] Jiangsu Engineering Laboratory of Light-Electricity-Heat Energy-Converting Materials and Applications, Changzhou University, Changzhou 213164, China

ARTICLE INFO

Article history:
Received 2 March 2022
Revised 26 March 2022
Accepted 18 April 2022
Available online 20 April 2022

Keywords:
Near-infrared emitter
Phosphorescence
Platinum complex
OLED
Operational lifetime

ABSTRACT

Due to the high decay rate of the non-radiative transition of long wavelengths, the molecular design of efficient and stable near-infrared (NIR) electroluminescent materials remains a big challenge. Herein, a new tetradentate cyclometalated platinum(II) complex with an N^C^C^N coordinated framework has been developed and used as a dopant for NIR organic light-emitting diodes (OLEDs). The complex exhibited a short-lived (0.5–1.5 μs) metal-to-ligand charge transfer (MLCT) excited state in doped and neat films. The resulting NIR OLEDs (λ_{EL} = 730 nm) achieved maximum external quantum efficiency (EQE_{max}) of 5.2% and radiance of 74626 mW sr^{-1} m^{-2}. Of note, the device exhibited excellent stability with operational lifetime of 119 h for LT_{90}. This work demonstrated the great potential of tetradentate platinum(II) complexes in the field of NIR OLEDs.

Near-infrared (NIR) emitters have shown great potential applications in organic light-emitting diodes (OLEDs), night vision, sensing, optical communications *etc*. [1–5]. However, the fast non-radiative transition of long-wavelengths governed by the energy gap law usually causes low luminescent efficiency [6,7]. For this reason, efficient NIR electroluminescent materials usually require a strong spin-coupling (SOC) effect and short excited state lifetime, *i.e*., a high utilization of triplet excitons and low non-radiation energy loss [1,8–10]. To date, several NIR emitters based on transition metal complexes have been widely developed due to their efficient phosphorescent emission characteristics [11–18]. However, most of the developed NIR emitting complexes are constructed from large substituents, increased π-conjugation length, additional heteroatoms/heterocycles, as well as the introduced additional donor-acceptor (D-A) units, which usually lead to significant difficulties in their synthesis [12,15,19,20]. In addition, although six-coordinated families, such as iridium(III), osmium(II) and ruthenium(III) complexes, can inhibit intermolecular aggregation, they also increase the molecular weight, which is not conducive to sublimation and purification [17,21–23]. When compared to the six-coordinated octahedral geometry, platinum(II) complexes with a four-coordinate square planar geometry form strong Pt-Pt interactions and exhibit unique photophysical properties, which are responsible for many key features, such as ligand to ligand charge transfer (LLCT), metal to ligand charge transfer (MLCT) and intramolecular ligand charge transfer (ILCT). As a result, several classes of phosphorescent platinum(II) complexes with high photoluminescence quantum yields (PLQYs), good color tunability, and high thermal stability have been explored as high performance NIR OLEDs [24–30].

Building molecules with electron-donating (D) and electron-accepting (A) units is the most efficient way to achieve NIR emission. The energy gap and electronic properties of these compounds can be readily and effectively tuned by controlling the structures of the D and A units [31–35]. Based on this strategy, several bidentate ligands have been reported to construct NIR emitting platinum(II) complexes. However, their intra-ligand (IL) excited state with metal perturbation limits their radiative decay rate in the order of 10^4 s^{-1} or smaller [1,36–38]. Therefore, a more rigid tetradentate ligand is desirable to suppress the non-radiative decay. The advantages of tetradentate platinum(II) complexes include: (i) avoiding energy loss *via* LLCT, improving the phosphorescent emission efficiency; (ii) inhibiting intramolecular vibration using a more rigid coordi-

* Corresponding authors.
E-mail addresses: zhangym@szu.edu.cn (Y. Zhang), jingshengmiao@szu.edu.cn (J. Miao), clyang@szu.edu.cn (C. Yang).

https://doi.org/10.1016/j.cclet.2022.04.043
1001-8417/

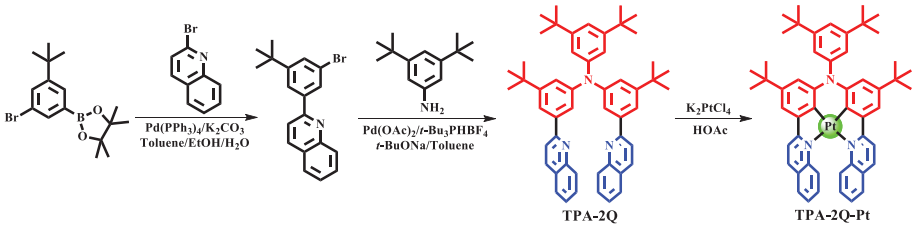

Scheme 1. Synthetic route of TPA-2Q-Pt.

nation plane,which further reduces non-radiative energy loss; and (iii) improving the stability.

Herein, we have designed a tetradentate platinum(II) complex (TPA-2Q-Pt) using triphenylamine (TPA) as a donor (D) and quinolone (Q) as an acceptor (A). The four *tert*-butyl groups on the TPA unit can improve the solubility, increase the electron-donating ability and inhibit intermolecular aggregation. In addition, the steric hinderance between the two quinoline units forms a distorted structure, which further reduces the intermolecular aggregation. Notably, remarkable NIR emission with peaks at 735 and 750 nm were observed for its dichloromethane solution and neat film, respectively. This complex exhibited efficient and short-lived NIR emissions from the $^{1/3}$MLCT states, which led to high performance OLEDs with maximum external quantum efficiencies of 5.2% and radiance of 74626 mW sr^{-1} m^{-2}. Of note, the device achieved appealing operational lifetimes (LT_{90}) of 119 h under a radiance of 5000 mW sr^{-1} m^{-2}.

TPA-2Q-Pt was prepared using a three-step method involving Suzuki coupling, Buchwald-Hartwig coupling and coordination reactions (Scheme 1). The complex was sublimated for purification under a pressure of $<10^{-4}$ Pa and temperature of ~280 °C. The complex was characterized using ^{1}H NMR spectroscopy, mass spectrometry, elemental analysis and single crystal X-ray diffraction studies (Fig. 1 and Table S1 in Supporting information), confirming its well-defined chemical structure. As shown in Fig. 1a, this complex presents a relatively twisted configuration: the movable benzene ring in TPA had a dihedral angle of ~84° with the coordination plane, and two quinolines in the same molecule also showed an angle of ~45° due to steric hindrance. There was no intermolecular Pt-Pt interaction. Intermolecular π-π stacking between two quinolines in different molecules were observed with distances of ~3.3 Å (Figs. 1b and c). Thermogravimetric analysis (TGA) under an N_2 atmosphere showed a high decomposition temperature (T_d) of 356 °C with 5% weight loss (Table 1 and Fig. S1 in Supporting information), which revealed the high thermal stability of the complex for the fabrication of OLEDs. Density functional theory (DFT) calculations revealed the MLCT and ILCT nature of their excited states. As expected, the HOMO was dominated by the platinum atom and TPA donor, and the LUMO was localized on the quinoline acceptors (Fig. S2 in Supporting information).

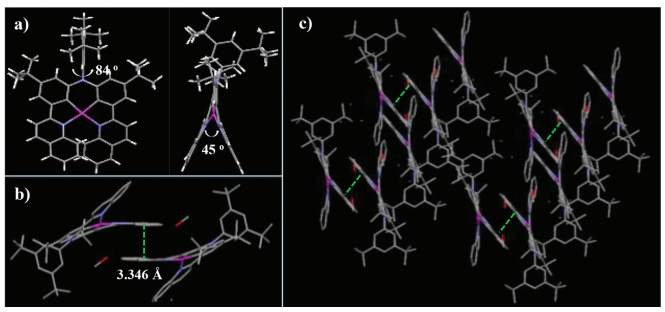

Fig. 1. X-ray crystal structures of TPA-2Q-Pt.

Table 1
Photophysical data for TPA-2Q-Pt.

λ_{em}[a] (nm)	τ[b] (μs)	τ[c] (μs)	Φ_p[d] (%)	k_r [e] (10^5 s^{-1})	k_{nr} [e] (10^5 s^{-1})	T_d[f] (°C)
735/711/755	0.49/0.72	1.4/1.6	15	1.1	6.1	356

[a] In deaerated dichloromethane (10^{-5} mol/L, left), 5 wt% PMMA doped film (middle) and neat film (right), respectively.
[b] In neat film after being aerated (left) and degassed (right).
[c] In 5 wt% PMMA doped film after being aerated (left) and degassed (right).
[d] Absolute photoluminescence quantum yield evaluated using an integrating sphere for the 5 wt% PMMA doped film after being degassed.
[e] Calculated using $k_r = \Phi/\tau$ and $k_{nr} = (1 - \Phi)/\tau$.
[f] The temperature at a weight loss of 5% under an N_2 atmosphere.

As shown in Fig. 2a, the cyclic voltammetry curve of TPA-2Q-Pt exhibited a reversible oxidation potential at 0.49 V versus ferrocene (Fc/Fc^+). The oxidation potential corresponded to the change in the distribution of the HOMO. The energy level of the HOMO (E_{HOMO}) was calculated to be –4.83 eV from the empirical relationship [39]. The energy level of the LUMO (E_{LUMO}) was further calculated to be –2.99 eV according to the energy level of the optical band gap. Fig. 2b depicted the UV-vis absorption and photoluminescence spectra of the TPA-2Q-Pt complex in dichloromethane. The intense absorption at <370 nm could be assigned to the spin-allowed π-π^* electronic transition. The next weaker absorption band at ~440 nm was ascribed to the singlet state of metal-to-ligand charge transfer (^{1}MLCT). The lowest absorption band at 500–700 nm with relatively small absorptivity originated from the enhanced transitions with ^{3}MLCT. In dichloromethane, TPA-2Q-Pt exhibited a broad, structureless photoluminescence with a peak at 735 nm. An obviously blue-shifted emission at 711 nm and red-shifted emission at 755 nm were observed in poly(methyl methacrylate) (PMMA) doped film (5 wt%) and neat film, respectively. This characteristic was consistent with the intermolecular π-π stacking. A PLQY of 15% was observed in the 5 wt% doped PMMA film, which was ascribed to its fast non-radiative decay mainly determined by the energy gap law [6,7]. Notably, the emission lifetimes were determined to be 0.49 and 0.72 μs for the aerated and degassed neat films, as well as 1.4 and 1.6 μs for the aerated and degassed for 5 wt% PMMA doped films, respectively, which verified the phosphorescent emission characteristics (Figs. 2c and d). The lifetime of the doped film is longer than that of the neat film due to the aggregation-caused concentration quenching. Consequently, the radiative transition rate (k_r) and non-radiative decay (k_{nr}) were calculated to be 1.1×10^5 and 6.1×10^5 s^{-1} for the 5 wt% PMMA doped film, respectively. Selected photophysical properties data are summarized in Table 1.

The electroluminescence (EL) properties of the complex were examined in a device structure comprised of ITO/HATCN (5 nm)/TPD15 (30 nm)/TCTA (15 nm)/DMIC-CZ + DMIC-TRZ: emitter (50 nm)/ANT-BIZ (30 nm)/Liq (2 nm)/Al (100 nm). The chemical structures and functions of 1,4,5,8,9,11-hexaazatripheny lene-hexacarbonitrile (HATCN), 4,4′-bis[*N*,*N*-di(1,1′-biphenyl-4-yl) amino]-1,1′-biphenyl (TPD15), tris(4-carbazolyl-9-ylphenyl)amine (TCTA), 5,7-dihydro-7,7-dimethyl-5-phenyl-3-(9-phenyl-9*H*-carba zol-3-yl)-indeno[2,1-*b*]carbazole (DMIC-CZ), 1,3-dihydro-1,1-di-

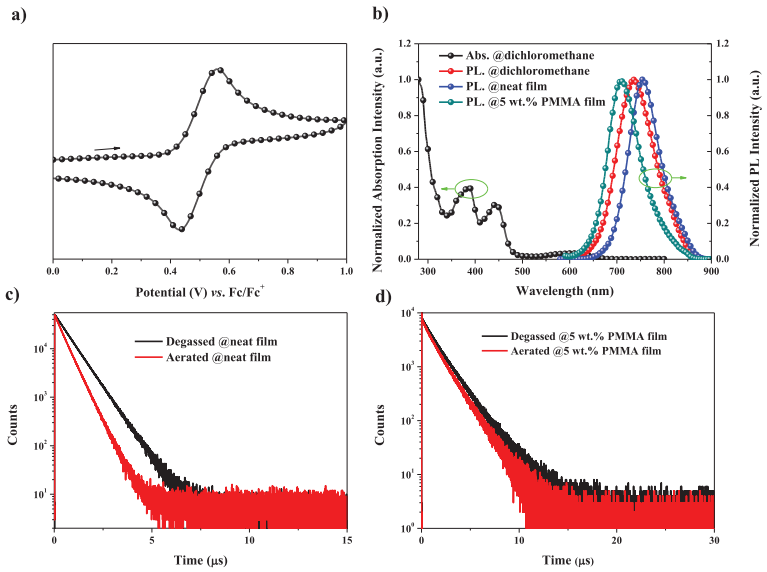

Fig. 2. (a) Cyclic voltammograms obtained for the complex films formed on a platinum electrode in an acetonitrile solution using 0.1 mol/L Bu_4NPF_6 and ferrocene as the electrolyte and internal standard. (b) Ultraviolet-visible absorption and photoluminescence spectra with an excitation wavelength of 485 nm. (c) PL decay characteristics of the neat film, and (d) 5 wt% PMMA doped film with an excitation wavelength of 485 nm.

methyl-3-(3-(4,6-diphenyl-1,3,5-triazin-2-yl)phenyl)-indeno-[2,1-*b*] carbazole (DMIC-TRZ) and 1-[4-(10-[1,1'-biphenyl]-4-yl-9-anthracenyl)phenyl]-2-ethyl-1*H*-benzimidazole (ANT-BIZ) are shown in Fig. S3 (Supporting information). Here, the HATCN, TPD15, TCTA, and ANT-BIZ are served as hole injection, hole transporting, electron blocking, and electron transporting layers, respectively. A mixture consisting of DMIC-CZ and DMIC-TRZ by co-evaporation was used as the exciplex host in order to obtain better device performance [40,41]. The device characteristics at various dopant concentrations are provided in Table 2, Table S2 and Fig. S4 (Supporting information). The maximum EQEs were decreased from 5.2% to 4.6% and 4.1% upon increasing the doping ratio from 3 wt% to 6 wt% and 9 wt%, which was attributed to the concentration quenching and triplet-triplet annihilation effect [42]. The related curves for the best-performing device (3 wt%) are also shown in Figs. 3a–c. The maximum EQE of the TPA-2Q-Pt based device was 5.2% with an electroluminescence peak at 730 nm and maximum radiance of 74626 mW sr^{-1} m^{-2}. Moreover, the EQEs at 1000, 5000 and 10,000 mW sr^{-1} m^{-2} were maintained at

Table 2
Key device data obtained for selected NIR OLEDs.

Concentrations	$\lambda_{EL,\ max}$ [a] (nm)	R_{max} [b] (mW sr^{-1} m^{-2})	EQEs [c] (%)	$CIE_{x,\ y}$ [d]
3 wt%	730	74626	5.2/5.1/4.6/4.0	0.65, 0.32
6 wt%	733	63308	4.5/4.4/4.1/3.5	0.70, 0.32
9 wt%	737	61186	4.1/4.0/3.6/3.4	0.68, 0.28

[a] Wavelength of the EL maximum.
[b] Maximum radiance.
[c] Maximum/@1000 mW sr^{-1} m^{-2}/@5000 mW sr^{-1} m^{-2}/@10000 mW sr^{-1} m^{-2}.
[d] Commission Internationalede L'Eclairage (CIE) coordinate @ EQE_{max}.

5.1%, 4.6% and 4.0%, respectively. To the best of our knowledge, the maximum EQE of 5.2% for TPA-2Q-Pt is among the highest NIR device efficiencies at wavelengths beyond 720 nm based on platinum(II) emitters without relying on intramolecular and/or intermolecular Pt-Pt interactions (MMLCT) [2,5,8,16,28].

The operational stability of this emitter was assessed in the same device structure (Fig. S3). The device was operated at a constant current of 2 mA, corresponding to an initial radiance of

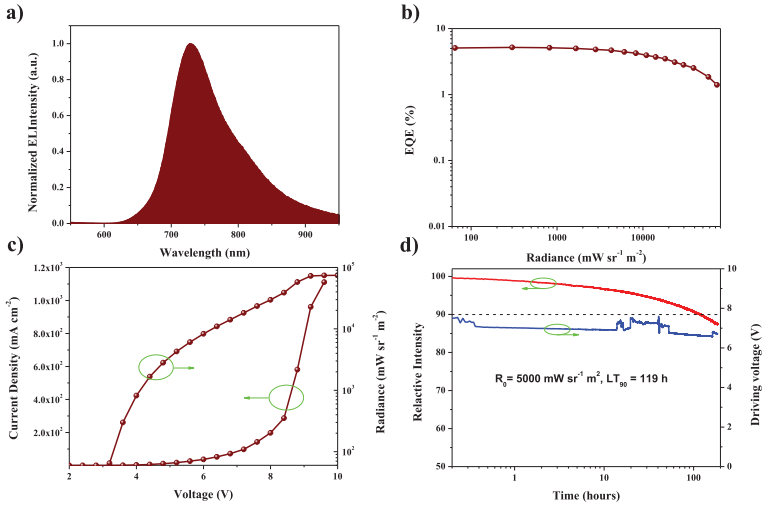

Fig. 3. (a) Normalized EL spectra. (b) EQE *versus* the radiance of the devices. (c) *J-R-V* characteristics. (d) Normalized EL intensity (left) and driving voltage (right) of the device versus operating time.

5000 mW sr^{-1} m^{-2}. As shown in Fig. 3d, the LT_{90} values (the time required for the luminance to drop to 90% of its initial value) was 119 h. By roughly assuming a moderate acceleration factor of 1.6, the LT_{90} at 1000 and 100 mW sr^{-1} m^{-2} were estimated to be 1562 and 62215 h, respectively, which represent the best stability for NIR OLEDs [8,43]. Notably, there was no obvious abrupt drop during operational period, which was different from the majority of previously reported device stability tests, and the driving voltage required by the device to maintain 2 mA was maintained at ~7 V, so that the device maintained a stable state without being broken-down.

To summarize, a novel platinum(II) complex exhibiting efficient NIR phosphorescence has been developed. The use of electron-donating TPA and electron-withdrawing quinolone guaranteed its long wavelength emission. The tetradentate coordination geometry confined the rigid structure and reduced non-radiation energy loss. The OLEDs based this complex showed high efficiencies, small efficiency roll-off, and excellent stability. This study provided a new strategy for the construction of novel NIR phosphorescent materials and demonstrated the potential application of tetradentate cyclometalated platinum complexes in NIR electroluminescent devices.

Declaration of competing interest

The authors declare that they have no known competing financial interests or personal relationships that could have appeared to influence the work reported in this paper.

Acknowledgments

This research was financially supported by the National Natural Science Foundation of China (Nos. 51903157 and 52130308), the Shenzhen Science and Technology Program (Nos. KQTD20170330110107046 and ZDSYS20210623091813040), and the School of Materials Science and Engineering, Jiangsu Engineering Laboratory of Light-Electricity-Heat Energy-Converting Materials and Applications (No. GDRGCS2021001). We thank the Instrumental Analysis Center of Shenzhen University for analytical support.

Supplementary materials

Supplementary material associated with this article can be found, in the online version, at doi:10.1016/j.cclet.2022.04.043.

References

[1] H. Xiang, J. Cheng, X. Ma, X. Zhou, J.J. Chruma, Chem. Soc. Rev. 42 (2013) 6128–6185.
[2] Y. Zhang, Y. Wang, J. Song, et al., Adv. Opt. Mater. 6 (2018) 1800466.
[3] J.O. Escobedo, O. Rusin, S. Lim, R.M. Strongin, Curr. Opin. Chem. Biol. 14 (2010) 64–70.
[4] V. Pansare, S. Hejazi, W. Faenza, R.K. Prud'homme, Chem. Mater. 24 (2012) 812–827.
[5] A. Zampetti, A. Minotto, F. Cacialli, Adv. Funct. Mater. 29 (2019) 1807623.
[6] G.H. Allen, R.P. White, D.P. Rillema, T.J. Meyer, J. Am. Chem. Soc. 106 (1984) 2613–2620.
[7] R. Englman, J. Jortner, Mol. Phys. 18 (1970) 145–164.
[8] Y. Zhang, J. Miao, J. Xiong, K. Li, C. Yang, Angew. Chem. Int. Ed. 61 (2022) e202113718.
[9] P. Jiang, J. Miao, X. Cao, et al., Adv. Mater. 34 (2022) e2106954.
[10] C.Y. Kuei, W.L. Tsai, B. Tong, et al., Adv. Mater. 28 (2016) 2795–2800.
[11] W. Xiong, F. Meng, C. You, et al., J. Mater. Chem. C 7 (2019) 630–638.
[12] C. You, D. Liu, J. Yu, et al., Adv. Opt. Mater. 8 (2020) 2000154.
[13] S. Kesarkar, W. Mroz, M. Penconi, et al., Angew. Chem. Int. Ed. 55 (2016) 2714–2718.
[14] J. Xue, L. Xin, J. Hou, et al., Chem. Mater. 29 (2017) 4775–4782.
[15] D. Ma, T. Tsuboi, Y. Qiu, L. Duan, Adv. Mater. 29 (2017) 1603253.
[16] K.T. Ly, R.W. Chen-Cheng, H.W. Lin, et al., Nat. Photonics 11 (2016) 63–68.
[17] X. Cao, J. Miao, M. Zhu, et al., Chem. Mater. 27 (2014) 96–104.
[18] J. Zhao, K. Yan, G. Xu, et al., Adv. Funct. Mater. 31 (2021) 2008325.
[19] Y. Zhang, F. Meng, C. You, et al., Dyes Pigm. 138 (2017) 100–106.
[20] Y. Zhang, Z. Yin, F. Meng, et al., Org. Electron. 50 (2017) 317.
[21] F. Wei, S.L. Lai, S. Zhao, et al., J. Am. Chem. Soc. 141 (2019) 12863–12871.
[22] M. Schulze, A. Steffen, F. Wurthner, Angew. Chem. Int. Ed. 54 (2015) 1570–1573.
[23] J. Liao, Y. Chi, S.H. Liu, et al., Inorg. Chem. 53 (2014) 9366–9374.
[24] G. Cheng, Q. Wan, W.H. Ang, et al., Adv. Opt. Mater. 7 (2018) 1801452.
[25] Y. Sun, C. Borek, K. Hanson, et al., Appl. Phys. Lett. 90 (2007) 213503.
[26] M. Chaaban, Y.C. Chi, M. Worku, et al., Inorg. Chem. 59 (2020) 13109–13116.
[27] X. Wu, D. Chen, D. Liu, et al., J. Am. Chem. Soc. 142 (2020) 7469–7479.
[28] P. Ganesan, W.Y. Hung, J.Y. Tso, et al., Adv. Funct. Mater. 29 (2019) 1900923.
[29] K. Zhang, T. Wang, T. Wu, et al., J. Mater. Chem. C 9 (2021) 2282–2290.
[30] S. Yang, F. Meng, X. Wu, et al., J. Mater. Chem. C 6 (2018) 5769–5777.
[31] G. Qian, Z. Zhong, M. Luo, et al., J. Phys. Chem. C 113 (2009) 1589–1595.
[32] G. Qian, Z. Zhong, M. Luo, et al., Adv. Mater. 21 (2009) 111–116.
[33] C. Li, R. Duan, B. Liang, et al., Angew. Chem. Int. Ed. 56 (2017) 11525–11529.
[34] U. Balijapalli, R. Nagata, N. Yamada, et al., Angew. Chem. Int. Ed. 60 (2021) 8477–8482.
[35] Z. Cai, X. Wu, H. Liu, et al., Angew. Chem. Int. Ed. 60 (2021) 23635–23640.
[36] T. Strassner, Acc. Chem. Res. 49 (2016) 2680–2689.
[37] Y. Sun, X. Yang, B. Liu, et al., J. Mater. Chem. C 7 (2019) 12552–12559.
[38] X. Yang, X. Xu, J. Zhao, et al., Inorg. Chem. 53 (2014) 12986–13000.
[39] C.M. Cardona, W. Li, A.E. Kaifer, D. Stockdale, G.C. Bazan, Adv. Mater. 23 (2011) 2367–2371.
[40] Y.S. Park, S. Lee, K.H. Kim, et al., Adv. Funct. Mater. 23 (2013) 4914–4920.
[41] Y. Seino, H. Sasabe, Y.J. Pu, J. Kido, Adv. Mater. 26 (2014) 1612–1616.
[42] B. Wang, F. Liang, H. Hu, et al., J. Mater. Chem. C 3 (2015) 8212–8218.
[43] L. Cao, J. Li, Z.Q. Zhu, L. Huang, J. Li, ACS Appl. Mater. Interfaces 13 (2021) 60261–60268.